09

Nd:YAG-based passive Q-switched laser for stainless steel surface cleaning

© M.D. Cheban[1], S.A. Filatova[1], Ya.V. Kravchenko[1], D.N. Mamonov[2], K.A. Scherbakov[2], S.M. Klimentov[2]

[1] Prokhorov Institute of General Physics, Russian Academy of Sciences, Moscow, Russia
[2] National Research Nuclear University „MEPhI", Moscow, Russia
E-mail: chebanmd@kapella.gpi.ru

Received February 28, 2025
Revised July 4, 2025
Accepted July 4, 2025

This paper presents the results of the development of a Nd:YAG-based passive Q-switched laser operating at a wavelength of 1064 nm. The laser generates pulses of 8 ns duration with an energy of 15.9 mJ. An optical fiber with a rectangular refractive profile, a core diameter of 600μm and a numerical aperture of 0.22 is used for radiation transmission. The efficiency of energy transfer through the fiber was 75%. The analysis of laser radiation parameters, conditions of its input into the fiber, as well as factors influencing losses and energy distribution in the optical system was carried out. The obtained results can be useful in the development of laser systems designed for cleaning and decontamination of metal surfaces.

Keywords: solid-state laser, Nd:YAG, passive Q-switching, multimode optical fiber.

DOI: 10.61011/TPL.2025.10.62107.20302

Decontamination of radiation-hazardous sites requires the removal of radioactive contaminants concentrated in the surface layer of materials [1–4]. Mechanical (grinding, blast cleaning) and chemical (acids, alkalies, surfactants) methods are used, but they produce radioactive waste, and proper disposal of that waste is a costly and technologically complex process.

Laser-plasma cleaning is free from these drawbacks [5,6]. Laser ablation causes melting, evaporation, and ionization of the material, and the melt is removed by vapor plasma pressure. In a liquid medium, cavitation provides an additional contribution [7]. The contributions of different mechanisms depend on the radiation parameters (primarily on the pulse duration).

Microsecond pulses induce strong heating and modification of the material [8,9], while femtosecond and picosecond pulses allow one to remove contaminants with minimum thermal impact [10], but devices generating such pulses are complex and expensive. Short nanosecond pulses (less than 10 ns) provide an optimum combination of cleaning efficiency, technological simplicity, and weak thermal influence [11,12].

Lasers with a wavelength of 1064 nm are used widely for cleaning. The absorption coefficient of steel at this wavelength is on the order of 15−30 % (depending on the angle of incidence, surface condition, and other factors [13,14]). A typical radiation source at this wavelength is an Nd:YAG-laser. It allows one to achieve a power density of $\sim 10^7$ W/cm^2 in nanolsecond pulses [15], which establishes the conditions needed for effective ablation.

Second-harmonic Nd:YAG lasers (532 nm) are also used for cleaning [16,17], since steel absorbs radiation at this wavelength more efficiently. However, such sources require nonlinear optical converters, which make the design more complex, reduce the energy efficiency, and increase the cost of the system. In practical tasks where reliability, simplicity, and versatility are critical, the 1064 nm wavelength remains a more viable option (especially in field and industrial decontamination tasks).

Nd:YAG lasers are in demand due to their high reliability, optical homogeneity of the active medium, and efficient heat dissipation. In the passive Q-switching mode with an Cr^{4+}:YAG crystal used as an absorber, such lasers (especially with transverse diode pumping) have the capacity to generate pulses shorter than 10 ns [18,19].

The mechanism of interaction between laser radiation and metal surfaces (specifically, stainless steel) differs significantly from the one found in selective cleaning of brittle or multilayer structures. At a wavelength of 1064 nm, the absorptance of certain contaminants (e. g., oxides or radionuclide sediments) may be comparable to or even lower than that of the metal substrate itself. Cleaning with nanosecond pulses often proceeds via thermomechanical impact: the pulse energy causes local evaporation of the material and the formation of subsurface pressure, which facilitates decontamination (aided also by the thermal response of the base material). With a proper choice of energy density, one may remove dense contaminants, such as persistent oxide films or radioactive deposits, efficiently. The thermal impact on the substrate is minimized in this case, and the damage to it is reduced accordingly.

The present study is aimed at constructing and optimizing a passive Q-switched Nd:YAG laser. The nanosecond mode was chosen for the technological simplicity and compactness

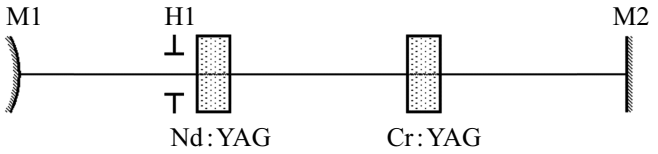

Figure 1. Optical circuit of the cavity (M1 — nontransmitting mirror, M2 — output mirror, Nd^{3+}:YAG — active element, Cr^{4+}:YAG — passive switch, and H1 — diaphragm).

of this arrangement and due to the need to ensure efficient ablation of contaminants while minimizing the depth of modification of the base material.

The results of preliminary experiments and data analysis were used to design a laser radiation source (Fig. 1) based on a single crystal of Nd^{3+}:YAG with transverse diode pumping (the crystal diameter was 5 mm, and its length was 60 mm). Radiation of three pulsed semiconductor diode arrays ($\lambda = 808$ nm) was directed to the active element from three sides, which ensured uniform distribution of optical pumping in the crystal volume, suppressed thermal gradients, and increased lasing stability. The pumping pulse duration was 250 μs, and the pulse repetition frequency was 100 Hz. The frequency was chosen with account for limitations on the power of diode pumping arrays and represents a compromise between achieving the required pulse energy and ensuring stable lasing in a given mode.

A passive switch based on an Cr^{4+}:YAG crystal (with an initial transmittance of 30 %) mounted at a small angle to the optical axis was used for Q-switching. This arrangement suppressed unwanted rereflections and the formation of a competing cavity, and coated surfaces minimized reflective losses. The switch was secured in a holder with a heat-conducting substrate providing passive cooling. This engineering solution helped stabilize the operation of the switch and prevent overheating that could affect its optical performance. The cavity design utilized an aperture diaphragm for spatial mode filtering, which provided an opportunity to form a high-quality output radiation beam.

Measurements of weak-signal gain for working radiation in a quantron were carried out to obtain a preliminarily estimate of the required density of mirrors. Probe radiation ($\lambda = 1064$ nm) from an Nd:YAG laser with a nanosecond pulse duration was passed through the quantron for this purpose. The maximum gain per pass in the used quantron (11.3) was achieved at a pumping power of 3 kW (diode array voltage, 120 V; current, 25 A).

A thermal lens, which affects the output parameters, forms in the active element of the laser during operation. Its strength depends on the pumping energy and the laser operating frequency. To stabilize the thermal lens, the laser was operated at constant parameters: a pulse repetition frequency of 100 Hz and a pumping power of 3 kW. Measurements with a He:Ne laser probe beam revealed that the thermal lens strength (focal length) at operating pump energies is $F \sim 1400$ mm. A convex nontransmitting mirror was used to improve the beam quality and increase the stability of lasing.

The energy and temporal characteristics of a laser pulse are shaped by a combination of factors influencing the lasing process. Among these are the cavity parameters, which include its length, the reflectivity of mirrors, and the alignment accuracy. The characteristics of the passive switch (initial transmittance, positioning relative to the optical axis, and saturation behavior) are also important. In addition, the pulse parameters are affected by the gain in the active medium, which depends on the pumping conditions. The spatial and modal features of generated radiation produce an additional contribution.

Table 1 characterizes the dependence of the pulse duration and energy on the reflection coefficient of output mirror M2. It is evident that the pulse duration and its energy increase as the reflection coefficient of output mirror M2 changes from 20 to 50 %. An increase in this reflection coefficient affects directly the Q factor of the cavity, extending the lifetime of a photon inside it. In the examined design, a higher reflection coefficient of the output mirror corresponds to a lower energy extracted from the cavity, but contributes to extension of the pulse by increasing the radiation accumulation time. At the same time, a mirror with a lower reflection coefficient requires higher gain in the active medium, which is limited by the available diode pumping power. According to calculated data, the optimum reflection coefficient is close to 43 %. However, having analyzed experimental data and factored in the stability of the system, we decided to use a mirror with a reflection coefficient of 50 %, which provides the best compromise between energy and duration of pulses.

An aperture diaphragm, which served for spatial filtering of modes and stabilizing the lasing process, was installed in the cavity. A variable aperture diameter provided an opportunity to control the mode composition of radiation and obtain a beam with improved spatial characteristics. A proper choice of diaphragm parameters made it possible to generate low-mode radiation that was matched well to the mode structure of the optical fiber, ensuring minimum input losses. The dependence of parameters of output radiation on the curvature radius of nontransmitting mirror M1 (1000−2500 mm) and the diaphragm diameter (2.6−3.4 mm) was also studied. The results are presented in Fig. 2. The error of measurement of the pulse energy and duration was ± 0.4 mJ and ± 0.2 ns, respectively. The resulting values were determined as standard deviations

Table 1. Dependence of the pulse energy and duration on the reflection coefficient of output mirror M2

Reflection coefficient of mirror M2	Pulse energy, mJ	Pulse duration, ns
20	8.65	7.2
35	11.5	7.5
50	15.7	21.3

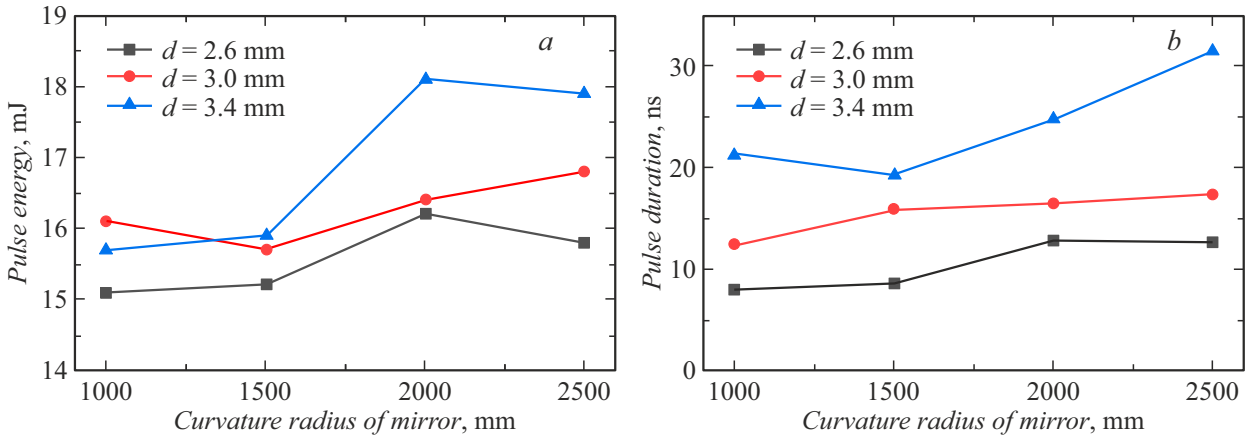

Figure 2. *a* — Dependence of the pulse energy on the curvature radius of nontransmitting mirror M1 at different diaphragm diameters; *b* — dependence of the pulse duration on the curvature radius of nontransmitting mirror M1 at different diaphragm diameters.

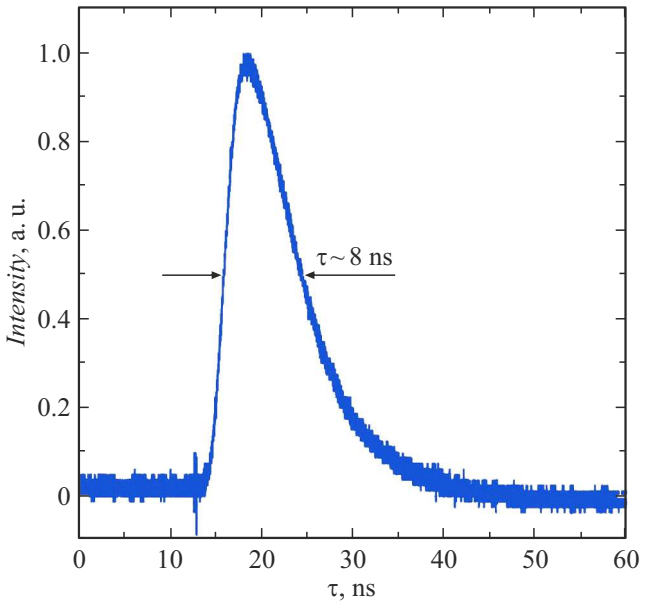

Figure 3. Temporal profile of a single 8 ns pulse.

based on five repeated measurements at each experimental point.

Matching the diameter of the aperture diaphragm to the curvature radius of nontransmitting mirror M1 allows for the formation of a stable generation region within the active element. Varying the parameters of this configuration, one may control the transverse mode dimensions and effectively suppress high-order modes, which has a positive effect on the pulse duration and energy and the spatial quality of radiation. We decided to use a nontransmitting mirror with a curvature radius of 1000 mm and a diaphragm of $d = 2.6$ mm. These parameters made it possible to obtain radiation with a pulse duration of 8 ns (Fig. 3) and a pulse energy of 15.9 mJ at the cavity output. The pulse repetition frequency was 100 Hz.

The pumping and generation parameters of the laser emitter with the chosen optimized optical cavity components are presented in Table 2. The quantitative beam quality parameter was $M^2 < 2$.

Since laser radiation is intended for cleaning the surface of materials, optical fiber was used for its convenient delivery to the processed object. Figure 4 presents a diagram of the laboratory prototype of a solid-state laser emitter based on Nd^{3+}:YAG. Laser radiation was coupled to a multimode fiber with numerical aperture $NA = 0.22 \pm 0.02$. Its silicon dioxide core had a diameter of 600 μm, while the fluorosilicate cladding diameter was 660 μm. The laser beam diameter at the waist was 120 μm. To avoid damage to the fiber end, the focus point was shifted inside the fiber to a distance of 3 mm from the end into which radiation was introduced. As laser radiation passed through the fiber, a number of modes formed, which propagated at different angles to the fiber axis at the output. This trend remained after focusing of radiation emerging from the fiber onto the sample surface, ensuring efficient penetration of radiation into narrow crevices, cavities, and irregularities.

Table 2. Parameters of the laboratory prototype of a solid-state Nd^{3+}:YAG laser with diode pumping

Parameter	Value
Pumping voltage, V	120
Pumping current, A	25
Diode array pumping power, W	3000
Cavity length, mm	138
Output mirror transmittance, %	50
Curvature radius of the nontransmitting mirror, mm	1000
Initial transmittance of the switch, %	30
Radiation wavelength, nm	1064
Diaphragm diameter, mm	2.6
Pulse duration, ns	8
Pulse energy, mJ	15.9
Pulse repetition frequency, Hz	100

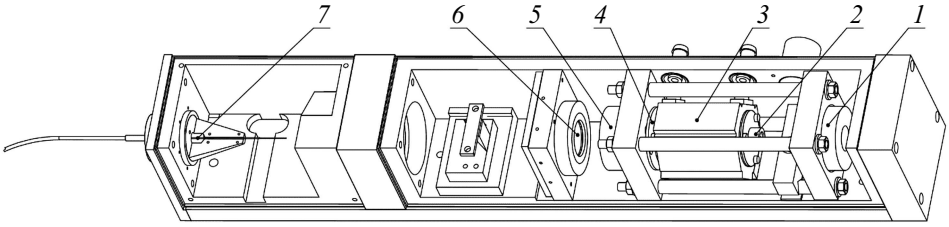

Figure 4. Laboratory prototype of a solid-state Nd^{3+}:YAG laser emitter. *1* — Nontransmitting mirror, *2* — diaphragm, *3* — quantron, *4* — passive switch, *5* — output mirror, *6* — focusing lens, and *7* — multimode fiber.

However, after 30 min of laser system operation, traces of degradation and destruction of the cladding (and then the core) were observed at a distance of 10 mm from the input end of the fiber. The end itself remained intact. This was indicative of leakage of certain higher order modes from the core into the cladding. To suppress this effect, the polymer cladding was stripped off [20]: it was removed from the input section of the fiber (~ 20 mm from the end), which remained in free space out of contact with holders or other structural elements. It is recommended to remove „parasitic" modes within the shortest possible input section to prevent their uncontrolled propagation. Although this reduces the efficiency of energy transmission, the service life of the system increases significantly. The conducted research allowed us to raise the efficiency of radiation input into the fiber approximately to 75 %. Failure tests, which included continuous operation of the fiber line for several hours (4 h per session), were carried out. The total operating time of the system without any signs of destruction of the fiber end or degradation of parameters exceeded 120 h in a series of applied experiments on laser cleaning. These results indicate a sufficient level of stability of the examined design solution under laboratory operating conditions.

A laboratory prototype of a solid-state Nd^{3+}:YAG laser with diode pumping and passive Q-switching by a switch based on an Cr^{4+}:YAG crystal was designed and fabricated. The dependences of the laser output parameters on the optical cavity components were investigated. The output radiation parameters (pulse energy and duration) were optimized. The output characteristics of the laboratory laser system prototype were as follows: wavelength, 1064 nm; pulse energy at the fiber output, 11.9 mJ; pulse duration, ~ 8 ns; pulse repetition frequency, 100 Hz. These parameters are promising for laser cleaning, since they ensure efficient removal of contaminants and oxide films without any significant thermal impact on the base.

The pulse repetition frequency may be increased in the future by installing a higher-power quantron or a fiber amplifier stage to compensate for the reduction in energy of individual pulses with higher pumping and ensure stable lasing under increased load. An enhancement of repetition frequency will translate into an increase in average radiation power, opening up opportunities for the development of more efficient laser cleaning systems. Numerical modeling of thermal processes in the target during ablation under high-PRF lasing with the aim of assessment of allowed processing modes and prevention of undesirable thermal influences on the material being cleaned remains an important direction for further research. Achieving an optimum balance between the energy of individual pulses and their frequency could be a key step toward constructing a commercial prototype adapted for high-speed cleaning of various materials.

The designed laser source was used in a number of experiments on removal of coatings, which simulated radioactive contamination, from stainless steel 08Kh18N10T (AISI 321) in various gas (air, argon, and process vacuum) and liquid media (distilled water, acetone, isopropyl alcohol, and a polymerizing gel composition based on polyvinyl alcohol) [21,22]. Experiments on decontamination of real radiation-contaminated stainless steel surfaces in a polyvinyl alcohol medium were also carried out [22].

Conflict of interest

The authors declare that they have no conflict of interest.

References

[1] V. Kumar, R. Goel, R. Chawla, M. Silambarasan, R.K. Sharma, J. Pharm. Bioallied Sci., **2** (3), 220 (2010). DOI: 10.4103/0975-7406.68505
[2] S. Liu, Y. He, H. Xie, Y. Ge, Y. Lin, Z. Yao, M. Jin, J. Liu, X. Chen, Y. Sun, B. Wang, Sustainability, **14** (7), 4021 (2022). DOI: 10.3390/su14074021
[3] L. Zhong, J. Lei, J. Deng, Z. Lei, L. Lei, X. Xu, Prog. Nucl. Energy, **139**, 103854 (2021). DOI: 10.1016/j.pnucene.2021.103854
[4] A. Gossard, A. Lilin, S. Faure, Prog. Nucl. Energy, **149**, 104255 (2022). DOI: 10.1016/j.pnucene.2022.104255
[5] Q. Wang, F. Wang, C. Cai, H. Chen, F. Ji, C. Yong, D. Liao, Nucl. Eng. Technol., **55** (1), 12 (2023). DOI: 10.1016/j.net.2022.09.020
[6] G. Zhu, Z. Xu, Y. Jin, X. Chen, L. Yang, J. Xu, D. Shan, Y. Chen, B. Guo, Opt. Lasers Eng., **157**, 107130 (2022). DOI: 10.1016/j.optlaseng.2022.107130
[7] A. Kumar, M. Prasad, R.B. Bhatt, P.G. Behere, D.J. Biswas, Opt. Laser Technol., **100**, 133 (2018). DOI: 10.1016/j.optlastec.2017.10.005
[8] H. Zhao, Y. Qiao, S. Chen, Q. Zhang, Y. Zang, Phys. Scripta, **96**, 125103 (2021). DOI: 10.1088/1402-4896/ac1bf1

[9] A. Ignatov, V. Zhakhovsky, A. Merzlikin, N. Inogamov, J. Phys.: Conf. Ser., **1092**, 012051 (2018). DOI: 10.1088/1742-6596/1092/1/012051
[10] T. Harada, S. Spence, A. Margiolakis, S. Deckoff-Jones, R. Ploeger, A.N. Shugar, J.F. Hamm, K.M. Dani, A.R. Dani, Materials, **10** (2), 107 (2017). DOI: 10.3390/ma10020107
[11] L. Zhou, H. Zhao, Q. Zhang, Q. Wang, G. Ma, Y. Qiao, H. Wang, Appl. Opt., **63** (6), A32 (2024). DOI: 10.1364/AO.504968
[12] V.P. Veiko, A. Samohvalov, E.I. Ageev, Opt. Laser Technol., **54**, 170 (2013). DOI: 10.1016/j.optlastec.2013.05.015
[13] G. de la Rosa-Santana, J. Alvarez-Chavez, H. Morano-Okuno, A. Morales-Ramirez, E. Uribe, Opt. Photon. J., **6** (10), 275 (2016). DOI: 10.4236/opj.2016.610028
[14] X. Li, T. Huang, A.W. Chong, R. Zhou, Y.S. Choo, M. Hong, Opto-Electron. Eng., **44** (3), 340 (2017). DOI: 10.3969/j.issn.1003-501X.2017.03.009
[15] S. Garnov, V. Konov, T. Kononenko, V. Pashinin, M. Sinyavsky, Laser Phys., **14**, 910 (2004).
[16] H.-J. Won, S.-H. Jung, C.-H. Jung, B. Choi, J.-K. Moon, K. Lee, Asian J. Chem., **24**, 4136 (2012).
[17] H.A. M. Afifi, M. Abdel-Ghani, R. Mahmoud, F.H. Alkallas, A.B.G. Trabelsi, A.M. Mostafa, Micromachines, **14**, 1415 (2023). DOI: 10.3390/mi14071415
[18] Y. Zhou, X. Li, H. Xu, R. Yan, Y. Jiang, R. Fan, D. Chen, Opt. Express, **29** (11), 17201 (2021). DOI: 10.1364/OE.425586
[19] Y. Jiang, M. Nie, R. Guo, X. Fu, Q. Liu, Opt. Laser Technol., **129**, 106276 (2020). DOI: 10.1016/j.optlastec.2020.106276
[20] S. Campbell, O. Blomster, M. Pålsson, Proc. SPIE, **7578**, 75781R (2010). DOI: 10.1117/12.842633
[21] M. Cheban, S. Filatova, Y. Kravchenko, K. Scherbakov, D. Mamonov, S. Klimentov, M. Savinov, M. Chichkov, Nucl. Eng. Technol., **56** (7), 2775 (2024). DOI: 10.1016/j.net.2024.02.039
[22] M. Cheban, K. Scherbakov, D. Mamonov, P. Parabin, S. Filatova, Ya. Kravchenko, S. Klimentov, M. Chichkov, Nucl. Eng. Technol., **57** (8), 103569 (2025). DOI: 10.1016/j.net.2025.103569

Translated by D.Safin